

2

OFFICE OF NAVAL RESEARCH

Contract N00014-86-K-0497

R&T Code 4132013

Technical Report No. 7

Compression Molded Polyurethane Block Copolymers.
I. Thermal and Thermomechanical Properties

by

J. T. Koberstein, A. F. Galambos, and L. M. Leung

Prepared for Publication

in

Macromolecules

University of Connecticut
Institute of Materials Science
and Department of Chemical Engineering
Storrs, CT 06269-3136

March 27, 1990

Reproduction in whole or in part is permitted for
any purpose of the United States Government

This document has been approved for public release
and sale; its distribution is unlimited

90 04 03 007

AD-A220 068

DTIC
ELECTE
APR 03 1990
S D

REPORT DOCUMENTATION PAGE

1a REPORT SECURITY CLASSIFICATION Unclassified			1b RESTRICTIVE MARKINGS None	
2a SECURITY CLASSIFICATION AUTHORITY			3 DISTRIBUTION/AVAILABILITY OF REPORT Approved for Public Release, Distribution Unlimited	
2b DECLASSIFICATION/DOWNGRADING SCHEDULE				
4 PERFORMING ORGANIZATION REPORT NUMBER(S) Technical Report #7			5 MONITORING ORGANIZATION REPORT NUMBER(S)	
6a NAME OF PERFORMING ORGANIZATION University of Connecticut		6b OFFICE SYMBOL (if applicable)	7a NAME OF MONITORING ORGANIZATION ONR	
6c ADDRESS (City, State, and ZIP Code) Storrs, CT 06269-3136			7b ADDRESS (City, State, and ZIP Code) 800 North Quincy Avenue Arlington, VA 22217	
8a NAME OF FUNDING/SPONSORING ORGANIZATION ONR		8b OFFICE SYMBOL (if applicable)	9 PROCUREMENT INSTRUMENT IDENTIFICATION NUMBER	
8c ADDRESS (City, State, and ZIP Code) 800 North Quincy Avenue Arlington, VA 22217			10 SOURCE OF FUNDING NUMBERS	
			PROGRAM ELEMENT NO	PROJECT NO
11 TITLE (Include Security Classification) Compression Molded Polyurethane Block Copolymers. I. Thermal and Thermomechanical Properties				
12 PERSONAL AUTHOR(S) J. T. Koberstein, A. F. Galambos, and L. M. Leung				
13a TYPE OF REPORT Technical		13b TIME COVERED FROM _____ TO _____	14 DATE OF REPORT (Year, Month, Day) 1990, 3, 27	15 PAGE COUNT
16 SUPPLEMENTARY NOTATION Prepared for publication in Macromolecules				
17 COSATI CODES			18. SUBJECT TERMS (Continue on reverse if necessary and identify by block number)	
FIELD	GROUP	SUB-GROUP		
19 ABSTRACT (Continue on reverse if necessary and identify by block number) The thermal and thermomechanical properties of a series of compression molded MDI/BDO/PPO-PEO segmented polyurethane block copolymers are reported as a function of hard segment content. Correlations between these properties show that the hard microdomain morphology is continuous for hard segment contents exceeding ca. 40%. At high program temperature rates, DSC thermograms exhibit a single high temperature endotherm corresponding to the melting of an extended form of MDI/BDO crystal. Multiple endotherms are observed at low DSC scan rates. For high hard segment content specimens, catastrophic softening is coincident with the onset of the first high temperature endotherm. The primary softening point for materials with discrete hard microdomains occurs at the soft microphase T _g . The soft microphase T _g is a minimum for a hard segment content of 50%. The apparent hard microdomain T _g decreases monotonically with increasing hard content and is consistent with heat capacity data for the soft microphase T _g which indicates increased incorporation of soft segment material into the hard microdomain for higher hard segment content materials. <i>Li et al.</i>				
20 DISTRIBUTION/AVAILABILITY OF ABSTRACT <input checked="" type="checkbox"/> UNCLASSIFIED/UNLIMITED <input type="checkbox"/> SAME AS RPT <input type="checkbox"/> DTIC USERS			21 ABSTRACT SECURITY CLASSIFICATION	
22a NAME OF RESPONSIBLE INDIVIDUAL			22b TELEPHONE (Include Area Code)	22c. OFFICE SYMBOL

Compression Molded Polyurethane Block Copolymers.

I. Thermal and Thermomechanical Properties"

J. T. Koberstein⁺

A. F. Galambos⁺⁺

L. M. Leung⁺⁺⁺

Department of Chemical Engineering and Institute of Materials
Science, University of Connecticut, Storrs, CT 06269-3136

Accession For	
NTIS CRA&I	<input checked="" type="checkbox"/>
DTIC TAB	<input type="checkbox"/>
Unannounced	<input type="checkbox"/>
Justification	
By	
Distribution /	
Availability Codes	
Dist	Avail and/or Special
A-1	



⁺ To whom correspondence should be addressed; present address:

⁺⁺ Present address: Himont Research and Development Center, 800 Greenbank
Road, Wilmington, DE 19808

⁺⁺⁺ Present address: Department of Chemistry
Hong Kong Baptist College
224 Waterloo Road
Kln, Hong Kong

Abstract

The thermal and thermomechanical properties of a series of compression molded MDI/BDO/PPO-PEO segmented polyurethane block copolymers are reported as a function of hard segment content. Correlations between these properties show that the hard microdomain morphology is continuous for hard segment contents exceeding ca. 40%. At high program temperature rates, DSC thermograms exhibit a single high temperature endotherm corresponding to the melting of an extended form of MDI/BDO crystal. Multiple endotherms are observed at low DSC scan rates. For high hard segment content specimens, catastrophic softening is coincident with the onset of the first high temperature endotherm. The primary softening point for materials with discrete hard microdomains occurs at the soft microphase T_g. The soft microphase T_g is a minimum for a hard segment content of 50%. The apparent hard microdomain T_g decreases monotonically with increasing hard content and is consistent with heat capacity data for the soft microphase T_g which indicates increased incorporation of soft segment material into the hard microdomain for higher hard segment content materials.

relatively little progress has been made in constructing quantitative structure-property correlations for segmented polyurethanes.

In the series of papers that follow we present a comprehensive study of correlations between thermal and thermomechanical properties, thermal history, microdomain structure, and microphase mixing in segmented polyurethanes prepared from MDI, BDO, and poly(propylene oxide-ethylene oxide) (PPO-PEO) soft segments. These materials have already been subject to extensive analysis in our laboratories using a wide range of techniques including small-angle x-ray scattering^{6,33}, thermal analysis^{7,33-34}, solid state deuterium NMR^{35,36}, simultaneous differential scanning calorimetry (DSC)/synchrotron x-ray scattering³³ and Fourier transform infrared spectroscopy³⁷. This first paper in the series deals with correlations between thermal and thermomechanical properties.

Thermoanalytical techniques have provided a broad base of information on MDI/BD based polyurethanes. Bonart et al.⁹⁻¹¹, used different heat treatments to prepare specimens with either paracrystalline or true crystalline order. X-ray diffraction results were used to construct possible hard segment packing models based upon consideration of the formation of a physical crosslinking network of interurethane hydrogen bonds. DSC characterization revealed apparent melting endotherms for both materials, but a substantially higher melting temperature for the crystalline material. The small angle x-ray scattering profiles and heat distortion temperatures were also found to differ for the two materials, but structure-property correlations could not be made. Heat distortion in the paracrystalline material was associated with melting and dissociation of the physical crosslink network, however heat distortion occurred some 30°C below the melting point in the crystalline material.

Low temperature softening was found to occur at the soft microphase T_g , at temperatures above that of the pure soft segment T_g , due to the presence of disordered hard segments distributed within the soft matrix. High temperature softening has not been attributed to any single transition but has been reported to occur over a range of temperatures where multiple endotherms are observed^{9-10,20}. These multiple endotherms are sensitive to the annealing history and are not thoroughly understood at present. X-ray diffraction studies³⁹⁻⁴¹ have demonstrated that multiple endotherms in highly-oriented heat-set materials are correlated with transformations between extended and contracted hard segment crystalline polymorphs. Simultaneous SAXS-DSC experiments³³ have shown that partial disordering of the hard microdomains occurs during each of the endotherms consistent with the softening behavior. Above the crystalline melting point, these polyurethanes disorder completely.

In what follows, we describe the thermoanalytical characterization of a set of compression molded polyurethane specimens differing in hard segment content. The results of this characterization are used to investigate correlations between thermal and mechanical transitions (i.e. soft and hard microphase glass transitions, heat distortion temperatures, multiple endotherms, and softening points) as well as their morphological origins.

II. Experimental

Materials

The materials studied are a series of segmented polyurethane block copolymers with varying hard segment content, denoted PU-XX, where XX represents the weight percent of hard segment units in the material. Hard segments consist of 4,4'-diphenylmethane diisocyanate (MDI) chain extended with 1,4 butane diol (BDO), while the soft segment is polyoxypropylene

(PPO-PEO) ($M_n=2000$, functionality = 1.94) end-capped with 30.4 weight percent polyoxyethylene. The polymers were prepared by a one-step polymerization with four percent excess MDI to ensure complete reaction, as described in the literature²⁴. Chemical compositions of the materials as well as some related physical properties are presented in Table 1. In addition to these materials, a hard segment end-capped polyol prepolymer, PU15 was prepared as a model polymer. Its properties are important to analyses that appear in later papers in this series. Specimens employed in this study have been reprecipitated from dimethyl formamide solutions of the "as received" polymers⁴², vacuum dried, and molded into 2 mm thick, 1.5 inch diameter disks at 180°C and 3000 psi pressure for 5 minutes under vacuum. These conditions were selected because they yielded materials which exhibit only a single melting endotherm (for high DSC heating rates), thus implying the existence of relatively simple morphologies compared to specimens exhibiting multiple endotherms. The chemical content of a selected molded specimen was verified as equivalent to that of the "as-received polymer" by elemental analysis. In addition, the solubility behavior of the material was unchanged by molding, and thermal properties were found to be reproducible upon thermal cycling. Based upon this evidence, we conclude that there is not any significant degradation of our specimens during molding; at least to any level which influences our results at present.

Differential Scanning Calorimetry

DSC data for all of the copolymers and the pure soft segment prepolymer were obtained with a Perkin-Elmer DSC-4 equipped with a model 3600 data station and calibrated with indium, cyclohexane, and sapphire standards. Characterization of the low temperature behavior of the specimens was accomplished by scanning at a rate of 20°C/min from -140°C to room temperature. Measurements were repeated ten to fifteen times with fresh

samples each time in order to establish statistical error limits on the values of the glass transition temperature (T_g) of the soft microphase and the change in heat capacity (ΔC_p) at that transition.

Thermal behavior above room temperature was investigated by scanning the specimens from 20 to 240°C at scan rates of 20 and 40°C/min. Values of peak maximum and onset temperatures, as well as fusion enthalpies of apparent hard segment melting endotherms, are reported.

Thermo-Mechanical Analysis (TMA)

Molded specimens were subjected to flexure and penetration probe analysis using a Perkin-Elmer thermomechanical analyzer (TMA-L0). Flexure tests were performed with an applied load of 66 psi at a scan rate of 5°C/min. Specimens were mounted on a quartz cantilever platform and scanned over two temperature ranges: -100 to 50°C, for detection of the soft microphase deflection point; and 30 to 170°C, for detection of the hard microdomain deflection temperature. The reported transition temperatures are the intersections of tangents drawn to the probe position versus temperature curve before and during deflection. Penetration probe tests were run on the molded materials with a probe load of 10 g, and were scanned from 0 to 220°C at a rate of 20°C/min. All reported transition temperatures were calibrated to the softening temperature of indium. As with the flexure studies, transition temperatures were taken as the intersection of tangents drawn to the probe position versus temperature curve in the region of interest.

Wide Angle X-ray Scattering (WAXS)

Wide angle x-ray scattering (WAXS) profiles of the molded disks were collected in the reflection mode using a Phillips goniometer. Nickel filtered $CuK\alpha$ radiation (wavelength = 0.1542 nm.) was produced by an XRG-3000 generator at an operating voltage of 40 KV and current of 20 mA.

The scattering intensity was monitored on a strip chart recorder as a function of the scattering angle (2θ) between 5 and 35 degrees using a goniometer arm speed of one degree per minute.

III. Results

Sub-ambient DSC

Low temperature DSC behavior (Figure 1) of the molded materials is typified by a single transition corresponding to the glass-to-rubber transition of the soft microphase. As the hard segment content of the specimens increases, the breadth of the transition region increases, while the magnitude of the observed change in heat capacity (ΔC_p) at the transition decreases, to the point of being indiscernable for the material containing 80 weight percent hard segment.

Onset and midpoint values of the soft microphase glass transition temperatures are reported as a function of sample composition in Figure 2. The dotted line represents a modified Fox relationship⁴³⁻⁴⁴ for the T_g 's of homogeneous copolymer systems that was reported in a previous study³⁴ (i.e., systems in which there is complete intersegmental mixing). Deviation of the experimental values of T_g from the Fox prediction occurs at hard segment weight fractions above 0.3, indicating a transition between a homogeneous and microphase separated morphology at this composition. This result is consistent with subsequent⁴⁵ and previous SAXS measurements⁶ which indicate that microdomain structure in specimens with less than 30% hard segment by weight is poorly developed if present at all. As the hard segment content increases beyond this critical value, the soft microphase T_g decreases to a local minimum for 50% hard segment. This result implies that the soft microphase is purest in PU50 and PU60. SAXS measurements⁶ of electron density variances also indicate that PU50 and PU60 possess the highest relative degree of microphase segregation.

The ΔC_p at T_g of the mixed soft microphase can be written as the sum of contributions from each of the constituents:

$$\Delta C_{p,mix} = W_{HS} \Delta C_{p^{\circ}HS} + W_{SS} \Delta C_{p^{\circ}SS} \quad (1)$$

where the subscripts HS and SS refer to hard and soft segment respectively, W_i is that portion of the total amount of species i in the material which resides within the soft microphase, and the superscript zero ($^{\circ}$) denotes pure component properties. It has been shown previously that $\Delta C_{p^{\circ}HS} \approx 0$ in the mixed microphase^{32,34}. It then follows that the fraction of soft segment residing in the soft microphase may be calculated from

$$W_{SS} = \Delta C_{p,mix} / \Delta C_{p^{\circ}SS} \quad (2)$$

Where $\Delta C_{p^{\circ}SS} = 0.194 \text{ cal/g}^{\circ}$ ³⁴. If W_{SS} is found to be less than the total weight fraction of soft segment in the polymer, it can be concluded that there is soft segment included within the hard microdomain.

The magnitude of the change in heat capacity at the soft microphase glass transition decreases monotonically with increasing hard segment content (see Figure 3 and Table 2). For all materials except PU20 the measured ΔC_p is equal to or less than that for complete microphase separation (i.e. the product of the pure polyol ΔC_p and the weight fraction of soft segment in the sample denoted by the solid line in Figure 3). The tendency for specimens with higher hard segment content to exhibit ΔC_p values below the ideal value indicates that some soft segment units are incorporated within the hard microdomain and interphase regions, and do not participate in the soft microphase glass transition process. This tendency is strongest for formulations with high hard segment content.

High Temperature DSC

DSC scans were also performed on the molded specimens over a temperature range of 0 to 240°C, at scan rates of 20 and 40°C/min. The results of the scans at differing rates indicate that high temperature endotherms

are sensitive to the DSC temperature program rate. At 40°C/min (Figure 4) specimens exhibit a single high temperature peak; in some cases accompanied by a smaller endotherm that exists as a "shoulder" on the main peak. At a scan rate of 20°C/min (Figure 5), however, all compositions with hard segment content above 40% exhibit distinct multiple endotherms. For these compression molded materials simultaneous wide angle x-ray diffraction/DSC experiments^{46,47} indicate that the multiple endotherms result from melting and immediate melt recrystallization of extended MDI/BDO crystals^{39,40,49}. Polymorphism⁴⁰ is not observed during the DSC scan, however, a contracted crystal form does develop upon cooling. Further details of this behavior are described in paper IV of this series⁴⁷. Observed peak temperatures (Table 3) are consistent with previous results for similar MDI/BD based polyurethanes^{27,28,30}. Since multiple endotherms result from melt-recrystallization during the DSC scan, we consider the 40°C/min data to be most appropriate to our analyses.

The single high temperature endotherms are asymmetric, being skewed towards lower temperatures. These shapes are consistent with what might be anticipated for specimens which are initially molded isothermally, followed by slow cooling. The majority of crystals form isothermally at the molding temperature. As the material cools however, additional material is able to crystallize due to the increased undercooling, giving rise to the skewed appearance of the endotherm.

The total enthalpy of the single high temperature endotherms apparent in the 40°C/min. data (Figure 4) increases linearly with hard segment weight fraction (Table 4) to an extrapolated enthalpy of ca. 11.5 cal/g for the pure hard segment. A value of 22.5 cal/g has been reported for a model compound containing three MDI residues exhibiting a similar melting temperature (208°C)³⁸.

Specimens with hard segment contents of 30% and above exhibit an apparent glass transition process that occurs in the range of 50-90°C (Table 5). The transition is not well defined, and is manifest as a small peak or change in slope of the DSC baseline. A hard microdomain glass transition is anticipated to occur in this temperature, but would be expected to give a more characteristic sigmoidal shape typical of that observed for the neat MDI/BDO copolymer. Previous DSC annealing studies on polyurethanes^{27,28,30,34} have also reported a weak endotherm of this nature, which has been referred to as an "annealing" or "room temperature annealing" peak, since it generally occurs about 20°C above the annealing temperature, T_a . Its origin has been ascribed to short range ordering of the hard segments.

Several reasons lead us to believe that, in the present case, the small transition apparent in the 50-59°C range for our compression molded specimens, reflects a hard microdomain T_g process. First of all, the specimens have been held at room temperature for an extended time period, the transitions occur at a temperature some 40-80°C higher. Previous annealing (i.e. melt crystallization) studies³⁴ gave peak melting temperatures, T_p , that were ca 20°C above T_a . Furthermore, $T_p - T_a$ was previously found to be an increasing function of hard segment content, whereas T_p for the molded specimens is a decreasing function of hard segment content. As the DSC scan rate increases, the magnitude of the apparent peak diminishes and the transition assumes a more sigmoidal appearance typical of a glass transition. The shape of the low scan data is consistent with what would be expected if the glass transition were followed immediately by a recrystallization exotherm. The overall shape would be a sigmoid followed by an exotherm, and would then look similar to a small endotherm. At higher rates, the recrystallization would be at a minimum such that the

sigmoidal shape characteristic of T_g would be predominant. The appearance of this feature is further emphasized by the apparent skewness of the endotherm due to the slow cooling process. Additional crystallization during slow cooling is only possible until the temperature reaches T_g , below which there can be no melting endotherm. This effect also tends to produce an apparent transition near T_g . The behavior is fully consistent with what is observed experimentally, and thus we conclude that the DSC transitions found in the 50-90°C range are reflective of an apparent hard microdomain T_g process. TMA results that follow also support this conclusion.

Values for ΔC_p and T_g midpoint for pure hard segment specimens quenched from the melt were determined by DSC to be 0.09 cal/g°C and 112°C (108°C onset), respectively. It is not possible to determine quantitative ΔC_p values for the apparent hard microdomain glass transition of the molded polyurethanes, however they are considerably smaller than would be calculated from the pure hard segment value. This is expected due to the presence of some degree of hard segment microcrystallinity and ordering, and as a result of inclusion of hard segments within the soft microphase as discussed earlier.

Thermo-Mechanical Analysis: Flexure Testing

Mechanical flexure tests were performed to determine heat distortion temperatures for each of the molded specimens. Distinct flexure occurred in specimens of low hard segment content in temperature regions corresponding to both the hard and soft microphase glass transitions.

In the case of PU20 and PU30, the flexure of the cantilevered specimens was catastrophic at the low temperature glass transition, reflecting the lack of a well developed, discrete hard segment domain morphology. The onset of low temperature flexure was in all cases coincident with observed DSC values for the soft microphase T_g (see Table 2 and Figure 6).

The flexure probe scan of PU-40 (Figures 6 and 7) shows two distinct heat distortion temperatures observed in the vicinity of the hard and soft microphase glass transition regions. This behavior is indicative of the development of a discrete hard microdomain structure within a soft microphase matrix.

Materials with hard segment contents of 50% and greater, do not exhibit appreciable flexure in the region of the soft microphase glass transition. Previous studies²⁴ also documented an absence of heat sag for materials in this composition range. Such behavior is consistent with the onset of a continuous hard microdomain structure at hard segment contents of 50% as was suggested by the results of SAXS analyses⁶.

High temperature flexure curves are shown in Figure 7. The heat distortion temperature (i.e., onset of flexure) for PU50 occurs at ca. 60°C and is coincident with the onset of the apparent hard microphase glass transition. For specimens of higher hard segment content a softening point is also detectable at the apparent hard microphase T_g (Table 5), however catastrophic distortion does not take place until much higher temperatures, near 160°C. Wide-angle x-ray scattering measurements that follow indicate that significant hard segment crystalline or para-crystalline order develops in these latter materials. If the crystalline microdomain structure is continuous, heat distortion is expected to be minimal until the three-dimensional network of ordered hard segment regions is disrupted at its melting temperature.

Thermo-Mechanical Analysis: Penetration Probe Testing

Typical penetration probe scans on the molded specimens appear in Figure 8. For all specimens two transition points are noted in the region between room temperature and 240°C: a change of slope in the probe position vs. temperature scan between 60-80°C; and complete penetration of the probe

indicating that hard segment ordering does not provide significant structural reinforcement for these low hard segment content polyurethanes at elevated temperatures. For specimens with hard segment weight content of 50% and above, however, softening is coincident with the onset of high temperature DSC endotherms (Figure 5), supporting the evidence from flexure testing that these high-hard-segment-content molded specimens maintain mechanical integrity up to temperatures corresponding to the disruption of hard segment aggregates.

Wide Angle X-Ray Scattering (WAXS)

WAXS profiles of the molded specimens (Figure 10) are typified by a broad, amorphous scattering halo between 10 and 30 degrees of 2θ accompanied by diffuse crystalline scattering peaks for samples with higher hard segment content. Comparison of the location of these peaks with literature values^{4,12,13,39,49,50} indicates that the crystal form evident in the molded materials most closely matches that of the extended MDI/BDO crystal termed Type I by Briber and Thomas^{39,49}. The endothermic peak maximum observed by DSC (using data taken at 40°C/min. to avoid restructuring during the DSC scan) varies between 199 and 212°C, bracketing the observed Type I crystal melting point of 207°C reported by Briber and Thomas. At lower scan rates multiple endotherms are seen due to melt-recrystallization^{46,47}. Estimates of the fraction of crystallinity in each of the samples were obtained from WAXS analysis by comparing the area under the amorphous halo to the area under the crystalline peaks by the method outlined by Alexander⁵¹ for semi-crystalline polymers. The fractional crystallinities (from WAXS analysis) based on the mass of polymer and the mass of hard segment are presented with similarly based hard segment heats of fusion (from DSC analysis) in Table 4. The enthalpy of the single high

temperature DSC endotherm varies linearly with hard segment content, while the fractional crystallinity does not, reaching a maximum for PU70 and actually decreasing for PU80.

These trends are difficult to interpret directly for a number of reasons. First of all, the average hard segment length, and the distribution of hard segment lengths changes markedly with hard segment content (see Table 1). Previous studies on model hard segments³⁸ have shown that the heat of fusion is dependent on the hard segment length. It is doubtful that the model compounds and the polyurethane hard segments crystallize in identical fashion, but there, nonetheless, may be an effect of length (i.e. overall hard segment content) on the heat of fusion. In addition, there is no direct way to quantitatively estimate the degree of crystallinity by traditional WAXS analysis of these materials due to an inability to measure an appropriate amorphous halo. When the hard segments melt, they also undergo an order-disorder transition and spontaneously mix intimately with the soft segments³³. The amorphous halo of this melt state is significantly different from that of a non-crystalline microphase separated material⁴⁶. The latter WAXS pattern is the appropriate one to employ in the crystallinity calculation, but is generally unobtainable experimentally. The reported crystallinities are based upon the WAXS of the disordered melt and therefore cannot be considered as quantitative.

Summary Discussion

Thermal and thermomechanical properties have been measured for a series of compression molded MDI/BD/PPO-PEO segmented polyurethane block copolymers as a function of the overall hard segment content. At high heating rates, the DSC thermograms exhibit only a single endotherm suggesting that a single microdomain structure is manifest for each material. The

results of wide angle diffraction experiments are consistent with the predominance of the Type I^{39,49} or extended⁴⁰ crystal structure in the MDI/BDO hard segments. The degree of crystallinity of the hard segments reaches a maximum of ca. 22% for a polyurethane with hard segment content of 70%. At low heating rates, restructuring (i.e. melt recrystallization) occurs during the DSC scan leading to the observance of multiple melting endotherms.

Thermomechanical analyses indicate that a continuous hard microdomain structure is manifest for materials with hard segment content greater than 40-50%. For compositions below this threshold, catastrophic flexure is found to be coincident with the soft microphase T_g detected by DSC experiments. For compositions greater than this threshold, initial flexure does not occur until an apparent hard microdomain T_g is observed and catastrophic flexure does not occur until much higher temperatures (ca. 160°).

Penetration probe results reflect similar behavior. For materials with a discrete hard microdomain structure, initial softening is coincident with the apparent hard microdomain T_g . Materials with a continuous hard microdomain morphology, on the other hand, exhibit penetration probe position versus temperature profiles more characteristic of expansion probe experiments. A distinct increase in the rate of expansion provides further indication of an apparent hard microdomain glass transition temperature for these materials. In addition, catastrophic softening for materials of continuous hard microdomain morphology is coincident with the onset temperature of the first high-temperature endotherm, whereas softening occurs significantly below this temperature for compositions with discrete hard microdomains.

Apparent hard microdomain T_g 's determined by penetration probe TMA correspond closely to the occurrence of a small apparent endotherm in the

DSC thermogram. The hard microdomain T_g 's indicated by flexure probe TMA are lower by 10-25°C from the values determined by the other techniques (due to a lower scan rate), but exhibit the same trend with composition. The apparent hard microdomain T_g decreases more or less monotonically as the hard segment content increases, indicative of an augmentation in the amount of soft segment incorporated within the microdomain.

Soft microphase glass transition temperatures were determined by DSC and flexure probe TMA. For compositions below the hard segment continuity threshold, the values furnished by the two techniques are in good accord. For compositions above the threshold, the values indicated by TMA exceed significantly those values determined by DSC. The lowest soft microphase temperature is found for the polyurethane with hard segment content of 50%. This is consistent with our previous findings and interpretation⁶ that the highest degree of microphase separation is attained for this composition since packing constraints for lamellar hard microdomains are a minimum when the fractions of the two microphases are equivalent. The soft microphase T_g 's for materials with less than 40% hard segment can be fit with a modified Fox equation assuming a completely homogeneous morphology. The microdomain structure is therefore at best poorly developed in these materials. The ΔC_p at the soft microphase T_g decreases linearly with increase in hard segment content, but falls below the theoretical value, indicating that some of the soft segment material is resident within the hard segment. The deviation from the ideal value increases with increasing hard segment, consistent with the corresponding decrease in the apparent hard microdomain T_g . In the papers that follow, these thermal transition data are used in conjunction with small-angle x-ray scattering analyses to examine microdomain compositions in these polyurethanes.

Acknowledgements

The portion of this work carried out by one of the authors (LML) was supported by National Science Foundation grant DMR-81054612 provided by the Polymer Program of the Division of Materials Research. The other authors (JTK and AFG) acknowledge partial support by the Office of Naval Research. Much of this work was performed while the authors were associated with Princeton University, using thermal analysis equipment that was procured through NSF grant DMR-8206187. Finally, we wish to thank Dr. R. J. Zdrahala, formerly of the Union Carbide Corp., for supplying the materials.

Registry No. 34407-15-3, (MDI).(BD).(methyloxirane).(oxirane) (copolymer).

References

1. Bonart, R.; Muller, E. H., J. Macromol. Sci., Phys. 1974, B10, 177.
2. Bonart, R.; Muller, E. H., J. Macromol. Sci., Phys. 1974, B10, 345.
3. Schneider, N. S.; Desper, C. R.; Illinger, J. L.; King, A. O.; Barr, D., J. Macromol. Sci., Phys. 1975, B11, 527.
4. Van Bogart, J. W.; Gibson, P. E.; Cooper, S. L., J. Polym. Sci., Polym. Phys. Ed. 1983, 21, 65.
5. Koberstein, J. T.; Stein, R. S., J. Polym. Sci., Polym. Phys. Ed. 1983, 21, 1439.
6. Leung, L. M.; Koberstein, J. T., J. Polym. Sci., Polym. Phys. Ed. 1985, 23, 1883.
7. Abouzahr, S.; Wilkes, G. L.; Ophir, Z., Polymer 1982, 23, 1077.
8. Ophir, Z.; Wilkes, G. L., J. Polym. Sci., Polym. Phys. Ed. 1980, 18, 1469.
9. Bonart, R., J. Macromol. Sci.-Phys. 1968, B2(1), 115.
10. Bonart, R., Morbitzer, L., and Hentze, G., J. Macromol. Sci.-Phys. 1969, B3(2), 337.
11. Bonart, R., Morbitzer, L., and Muller, E. H., J. Macromol. Sci.-Phys. 1974, B9(3), 447.
12. Blackwell, J. and Gardner, H., Polymer 1979, 20, 13.
13. Blackwell, J. and Nagarajan, M., Polymer 1981, 22, 202.
14. Huh, D. S. and Cooper, S.L., Polym. Eng. Sci. 1971, 11, 369.
15. Koberstein, J. T., Ph.D. Dissertation, University of Massachusetts, Amherst, 1979.
16. Seymour, R. and Cooper, S. L., J. Polym. Sci. Polym. Lett. 1971, 9, 689.
17. Samuels, S. and Wilkes, G., J. Polym. Sci.-Polym. Phys. Ed., 1973, 11, 807.

18. Jacques, C., "Polymer Alloys, Blends, Blocks, Grafts, and Interpenetrating Networks" Eds. D. Klemperer and K. Frisch, Plenum Press, NY, 1977.
19. Senich, G. A.; MacKnight, W. J., Adv. Chem. Ser. 1979, 176, 97.
20. Brunette, C. M.; Hsu, S. L.; MacKnight, W. J.; Schneider, N. S., Polym. Eng. Sci. 1981, 21, 163.
21. Huh, D. S.; Cooper, S. L., Polym. Eng. Sci., 1971, 11, 369.
22. Ng, H.; Allegrezza, A. E.; Seymour, R. W.; Cooper, S. L., Polymer 1973, 14, 255.
23. Illinger, J. I.; Schneider, N. S.; Karasz, F. E., Polym. Eng. Sci., 1972, 12, 25.
24. Zdrahala, R. J.; Critchfield, F. E.; Gerkin, R. M.; Hager, S. L., J. Elastomers Plast. 1980, 12, 184.
25. Kajiyama, T.; MacKnight, W. J., Macromolecules, 1969, 2, 254.
26. Kajiyama, T.; MacKnight, W. J., J. Trans. Soc. Rheol. 1969, 13(4), 527.
27. Seymour, R. W.; Cooper, S. L., Macromolecules, 1973, 6, 48.
28. Hesketh, T. R.; Van Bogart, J. W. C.; Cooper, S. L., Polym. Eng. Sci. 1980, 20, 190.
29. Schneider, N. S.; Paik Sung, C. S. Matton, R. W. Illinger, J. L., Macromolecules 1975, 8, 62.
30. Van Bogart, J. W. C.; Bluemke, D. A.; Cooper, S. L., Polymer, 1981, 22, 1428.
31. Schneider, N. S.; Paik Sung, C. S., J. Polym. Sci., Polym. Chem. Ed. 1977, 17, 73.
32. Camberlin, Y.; Pascault, J. P., J. Polym. Sci., Polym. Chem. Ed. 1983, 21, 415.
33. Koberstein, J. T.; Russell, T. P., Macromolecules, 1986, 19, 714.

34. Leung, L. M.; Koberstein, J. T., *Macromolecules*, 1986, 19, 706.
35. Dumais, J. J.; Jelinski, L. W.; Leung, L. M.; Gancarz, I.; Galambos, A.; Koberstein, J. T., *Macromolecules*, 1985, 18, 116.
36. Kintantar, A.; Jelinski, L. W.; Gancarz, I.; Koberstein, J. T., *Macromolecules*, 1986, 19, 1876.
37. Koberstein, J. T.; Gancarz, I.; Clarke, T. C., *J. Polym. Sci. Polym. Phys. Ed.* 1986, 24, 2487.
38. Camberlin, Y., Pascault, J. P., Letoffe, M., and Claudy, P., *J. Polym. Sci.-Polym. Chem. Ed.* 1982, 20, 383.
39. Briber, R. M.; Thomas, E. L., *J. Macromol. Sci., Phys.* 1983, B22(4), 509.
40. Blackwell, J.; Lee, C. D., *J. Polym. Sci., Polym. Phys. Ed.* 1984, 22, 759.
41. Macosko, C. W., private communication.
42. Leung, L. M., Ph.D. Dissertation, Princeton University, 1985.
43. Wood, L.A., *J. Polym.Sci.* 1958, 28, 319.
44. Fox, T. G., *Bull. Am. Phys. Soc.* 1956, 50, 549.
45. Leung, L. M.; Koberstein, J. T., *Macromolecules*, to be published.
46. Galambos, A. F., PhD Dissertation, Princeton University, 1989.
47. Koberstein, J. T.; Galambos, A. F., *Macromolecules*, to be published.
48. Cohen, R. E.; Ramos, A. R., *Macromolecules*, 1979, 12, 131.
49. Briber, R. M.; Thomas, E. L., *J. Polym. Sci. Polym. Phys. Ed.*, 1985, 23, 1915.
50. Born, L.; Crone, J.; Hespe, H.; Muller, E. H.; Wolf, K. H., *J. Polym. Sci. Polym. Phys. Ed.* 1984, 22, 163.
51. Alexander, L. E., "X-Ray Diffraction Methods in Polymer Science", Wiley Interscience, NY, 1969.

List of Figures

- Figure 1. Sub-ambient DSC of molded samples; scan rate of 20°C/min.
- Figure 2. Soft microphase glass transition temperatures as a function of composition. Triangles represent Tg onset temperatures while the circles indicate midpoint Tg values. The dotted line represents the behavior (i.e. Tg midpoints) expected for homogeneous specimens in the absence of microphase separation³⁴.
- Figure 3. Change in specimen heat capacity at the soft microphase Tg as a function of sample composition.
- Figure 4. High-temperature DSC of molded samples; scan rate of 40°C/min.
- Figure 5. High-temperature DSC of molded samples; scan rate of 20°C/min. Down-arrows denote the the onset of the initial transition in penetration probe position; up-arrows signify the onset of catastrophic softening determined by penetration probe analyses performed at the same scan rate.
- Figure 6. TMA of molded samples: Sub-ambient flexure probe; scan rate of 5°C/min. Arrows indicate midpoint Tg values from DSC analysis (scan rate of 20°C/min).
- Figure 7. TMA of molded samples: High-temperature flexure probe; scan rate of 5°C/min. Arrows indicate hard microdomain Tg values from penetration probe analysis (scan rate of 20°C/min).
- Figure 8. TMA of molded samples: High-temperature penetration probe; scan rate of 20°C/min. Arrows indicate inflection points in slope of probe position vs. temperature plot.

Figure 9. DSC endotherm temperatures (from Fig. 5) and TMA softening points as a function of sample composition. Triangles represent penetration probe softening points, squares are the onset temperatures of Peak 1 DSC endotherms, circles denote the temperatures of the Peak 1 maxima, and diamonds are the temperatures of Peak 2 maxima. Materials to the right of the vertical line have a continuous hard microdomain morphology.

Figure 10. Wide-angle X-ray scattering profiles of molded specimens.

TABLE 1
Characteristics of Elastomers

Materials	Hard Segment		Number	Hard Segment
	wt. % (MDI+BDO)	Density (gm/cc)	Average MW* of Hard Seg. (gm/mole HS)	Theoretical Volume Fraction
PU-20	20	1.142	500	0.17
PU-30	30	1.165	800	0.26
PU-40	40	1.192	1200	0.35
PU-50	50	1.218	1700	0.45
PU-60	60	1.235	2300	0.55
PU-70	70	1.270	3100	0.66
PU-80	80	1.292	4300	0.77

*Calculated from the most probable distribution for a one-step polymerization

Table 2
Soft Microphase Glass Transition Data

Specimen	Glass Transition DSC		ΔC_p (Cal/g° C)	TMA
	Onset	Midpoint		Flexure Point (°C)
Polyo1	-71	-69	0.196	--
PU20	-51	-43	0.166	-45
PU30	-50	-41	0.131	-42
PU40	-52	-44	0.119	-44
PU50	-54	-44	0.092	-40
PU60	-53	-42	0.064	-37
PU70	-51	-35	0.039	--
PU80	--	--	--	--

Table 3
High Temperature Endotherm Temperatures (°C)

Specimen	DSC					TMA
	(40°C/min)		(20°C/min)			(20°C/min)
	Onset	Peak	Onset	Peak 1	Peak 2	Softening Point
PU30	187	199	172	196	214	140
PU40	200	207	198	207	222	172
PU50	189	202	190	202	212	196
PU60	189	201	190	201	214	195
PU70	200	212	200	206	215	203
PU80	194	204	196	205	219	199

Table 4
Fusion Enthalpy and Apparent Crystallinity

Specimen	Heat of Fusion (DSC)		Apparent % Crystallinity (WAXS)	
	cal/g-polymer	cal/g-hard segment*	(polymer)	(hard segment)*
PU30	0.4	1.3	0	0
PU40	1.5	3.8	3.7	9.3
PU50	3.2	6.4	7.2	14.4
PU60	4.8	8.0	9.3	15.5
PU70	6.6	9.4	15.5	22.1
PU80	8.2	10.3	13.4	16.7

* assuming complete microphase separation.

Table 5
Apparent Hard Microdomain Glass Transition Temperatures (°C)

Specimen	TMA		DSC
	Flexure Probe ⁺	Penetration Probe ⁺⁺	Peak ⁺⁺
PU30	--	91	92
PU40	72	83	87
PU50	60	82	86
PU60	46	78	77
PU70	46	73	70
PU80	47	70	61

⁺ scan rate of 5°C/min

⁺⁺ scan rate of 20°C/min

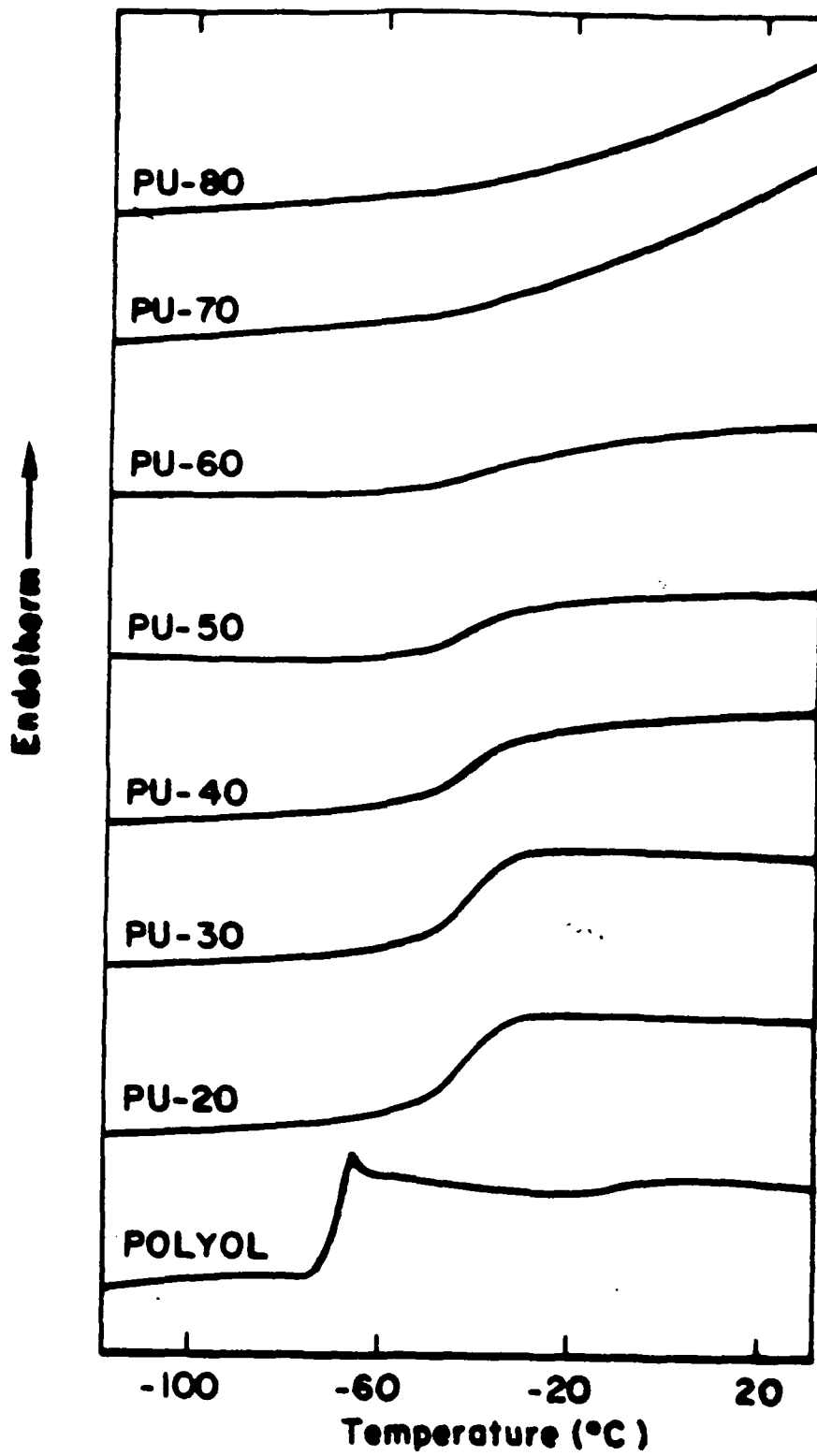


Fig. 1

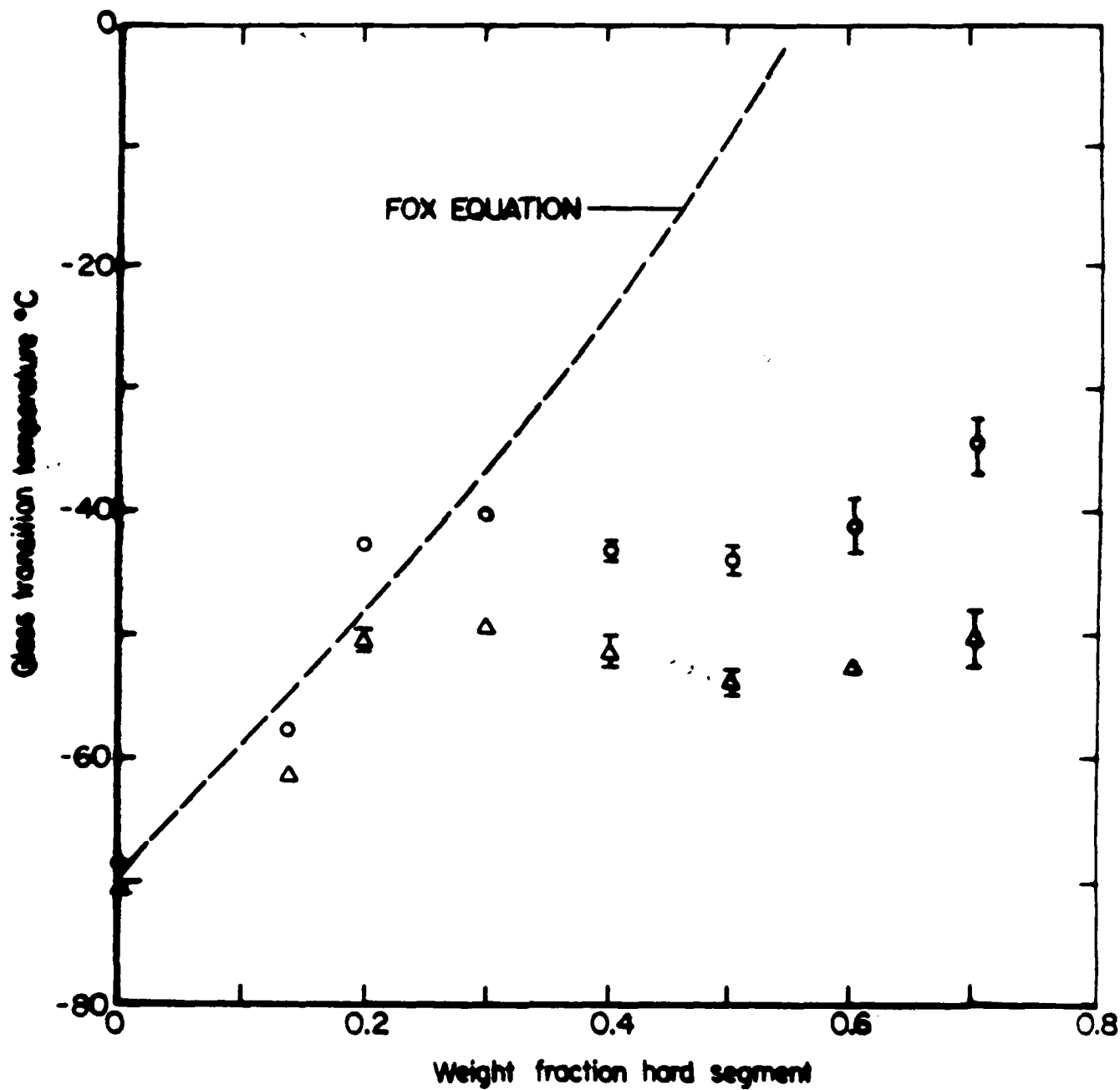


Fig. 2

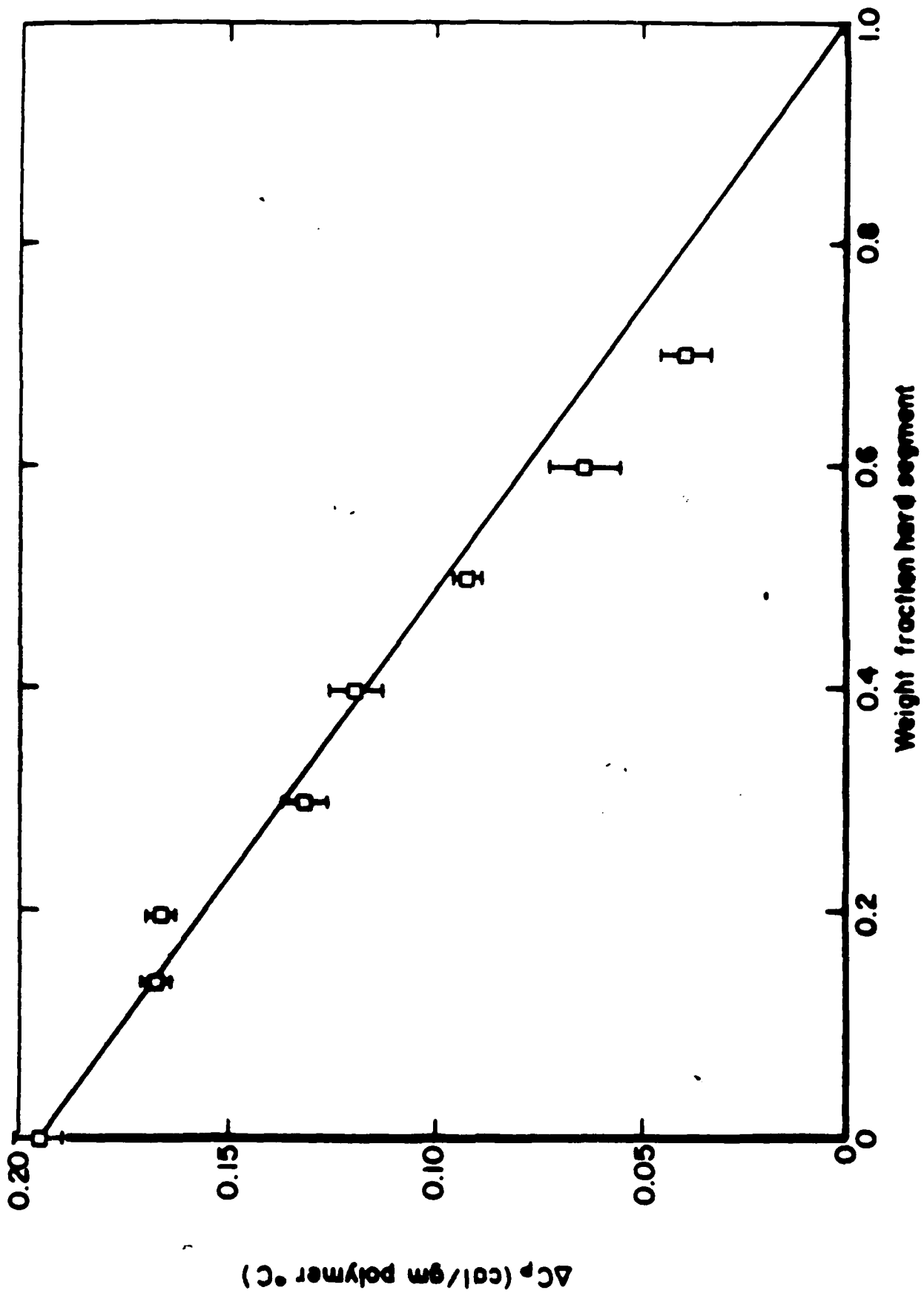


Fig 3

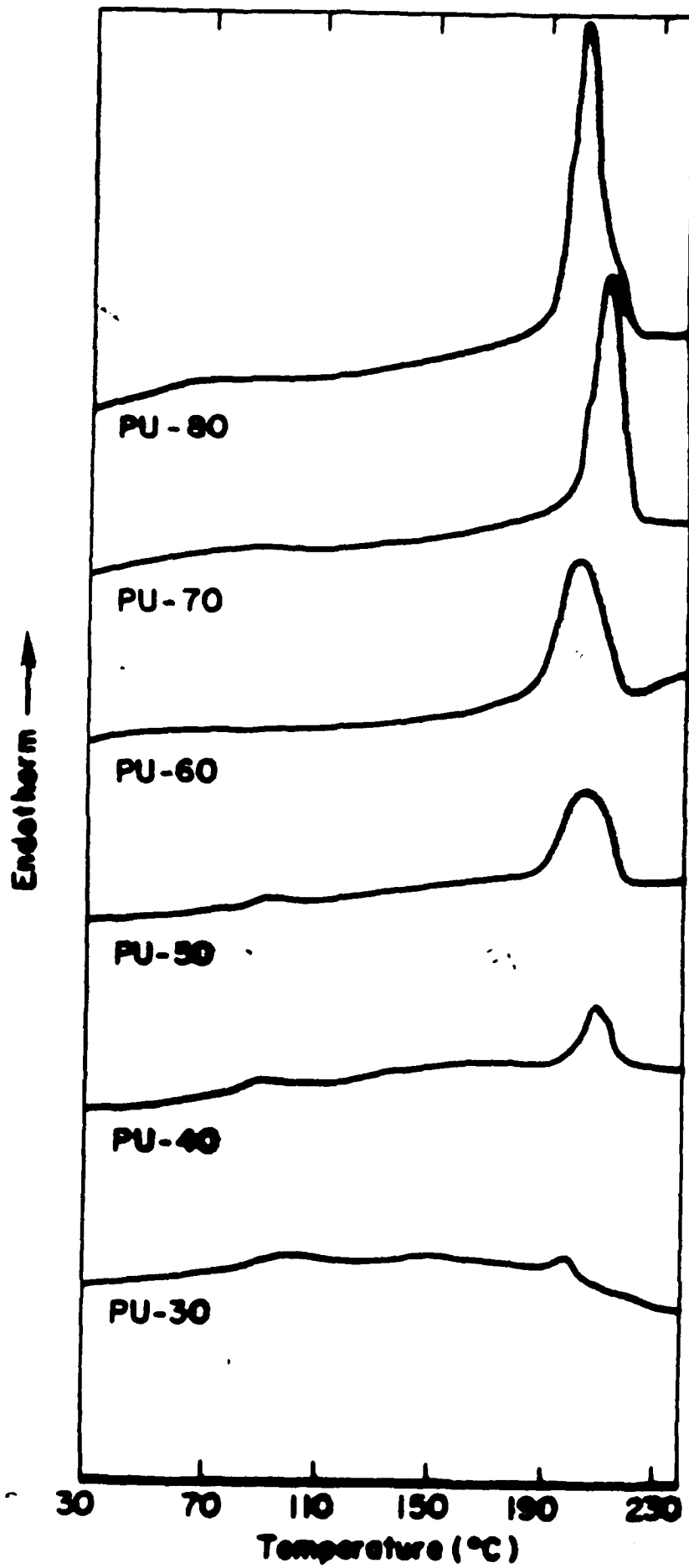


Fig 4

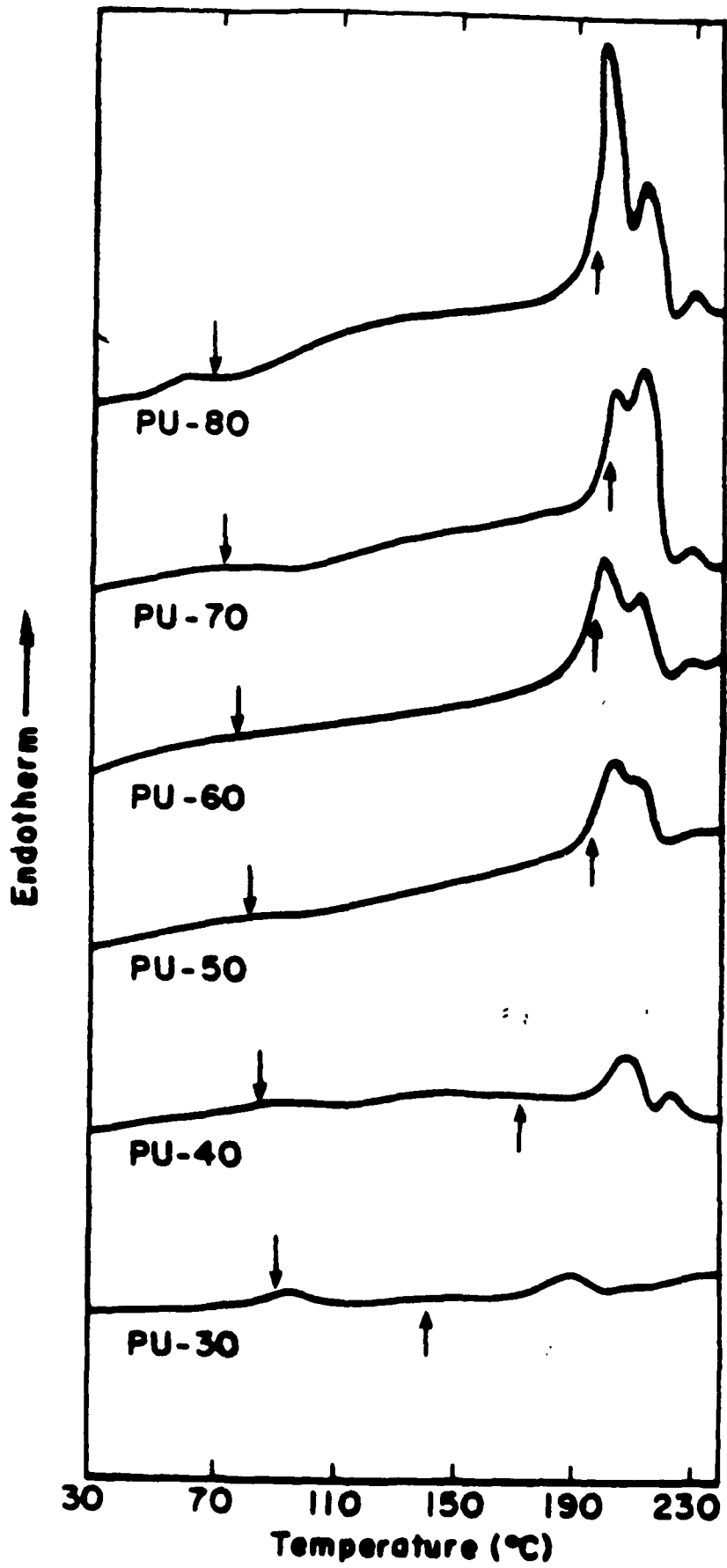


Fig 5

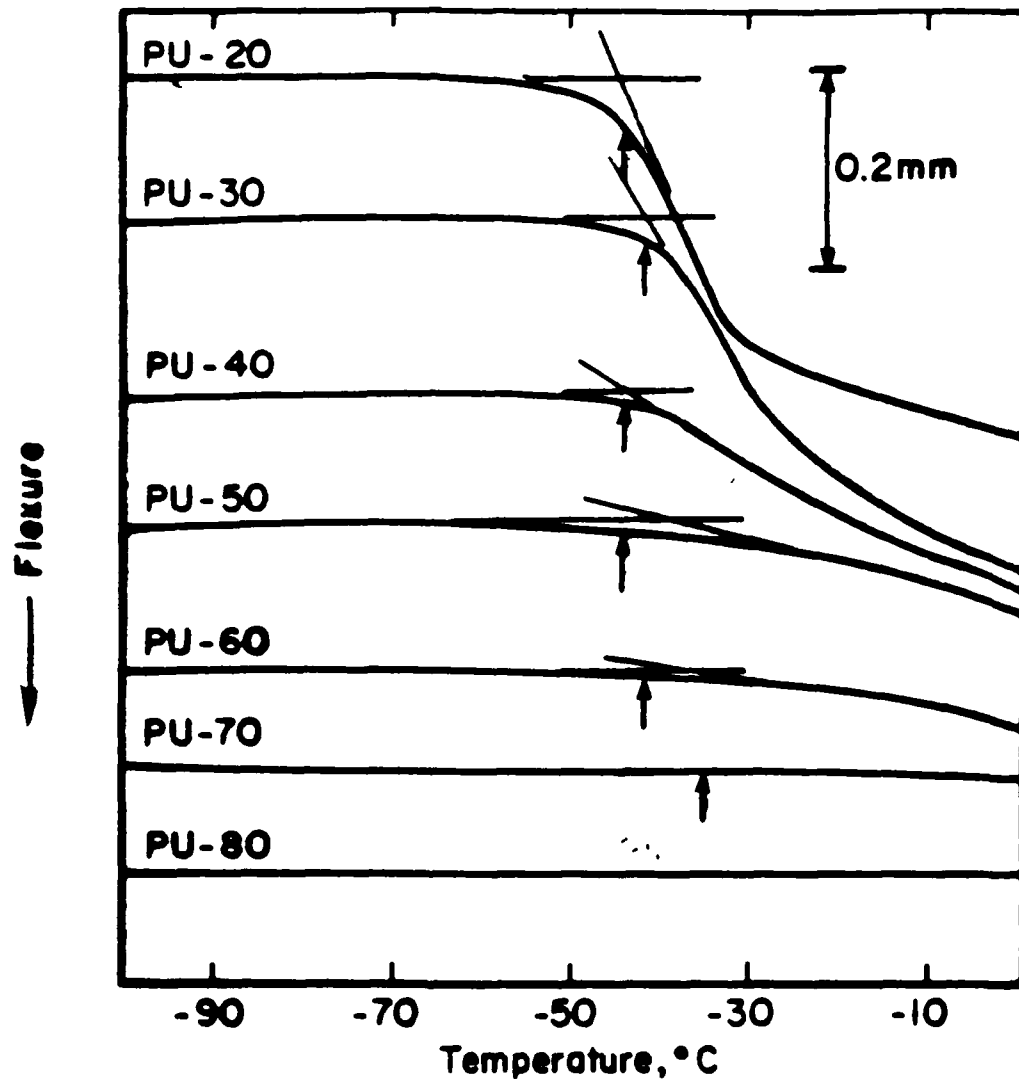


Fig 6

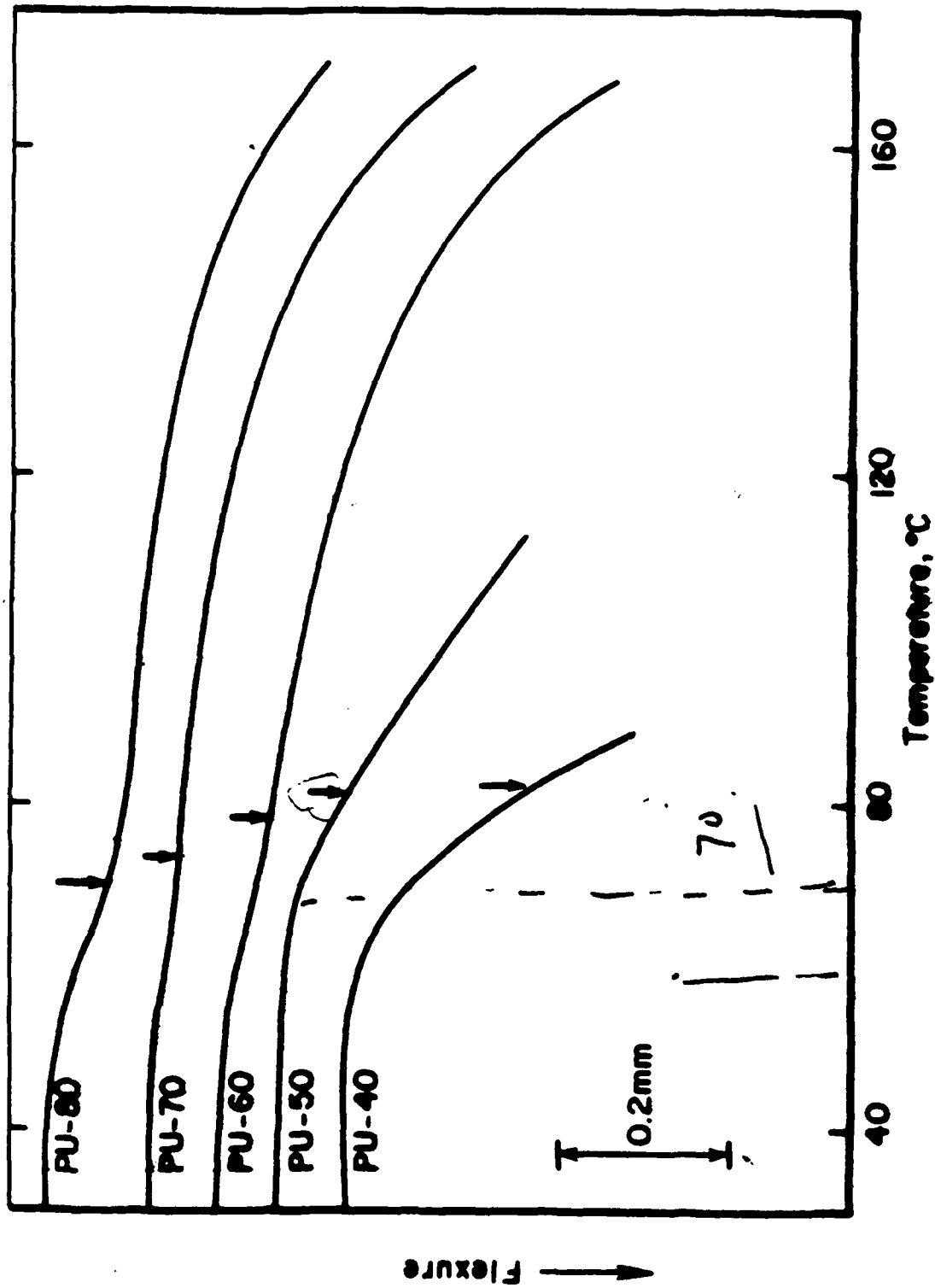


Fig 7

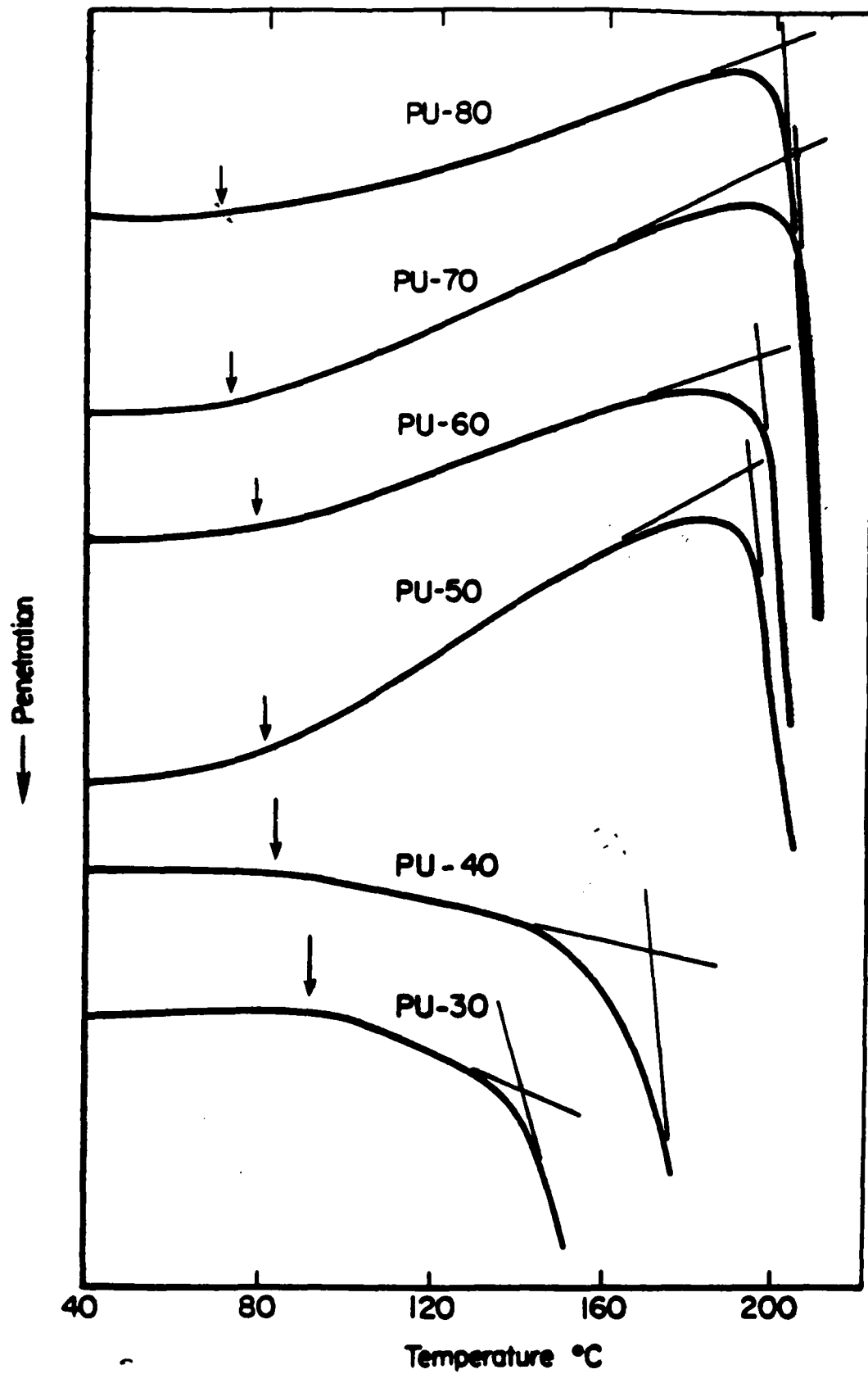


Fig 8

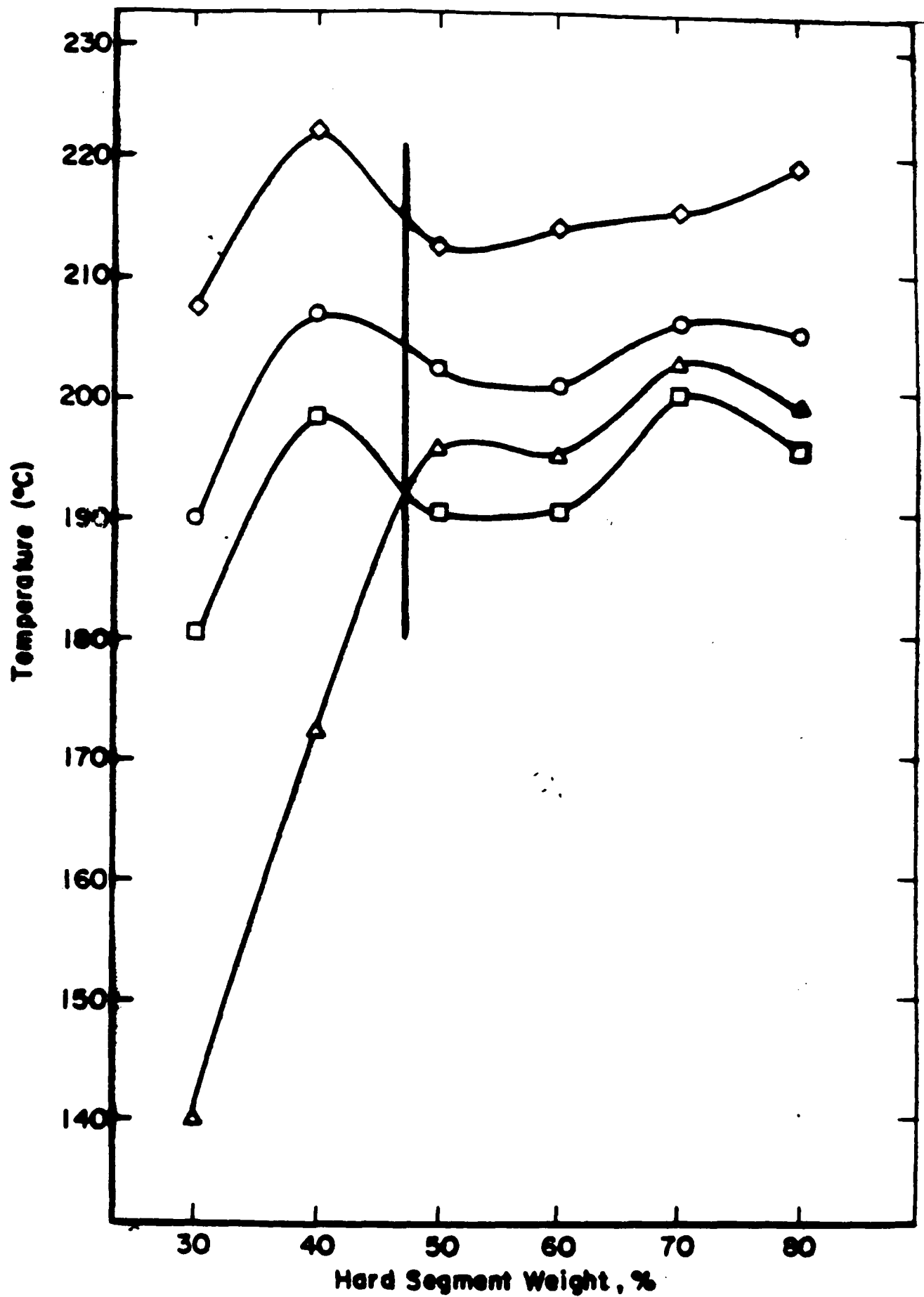


Fig 9

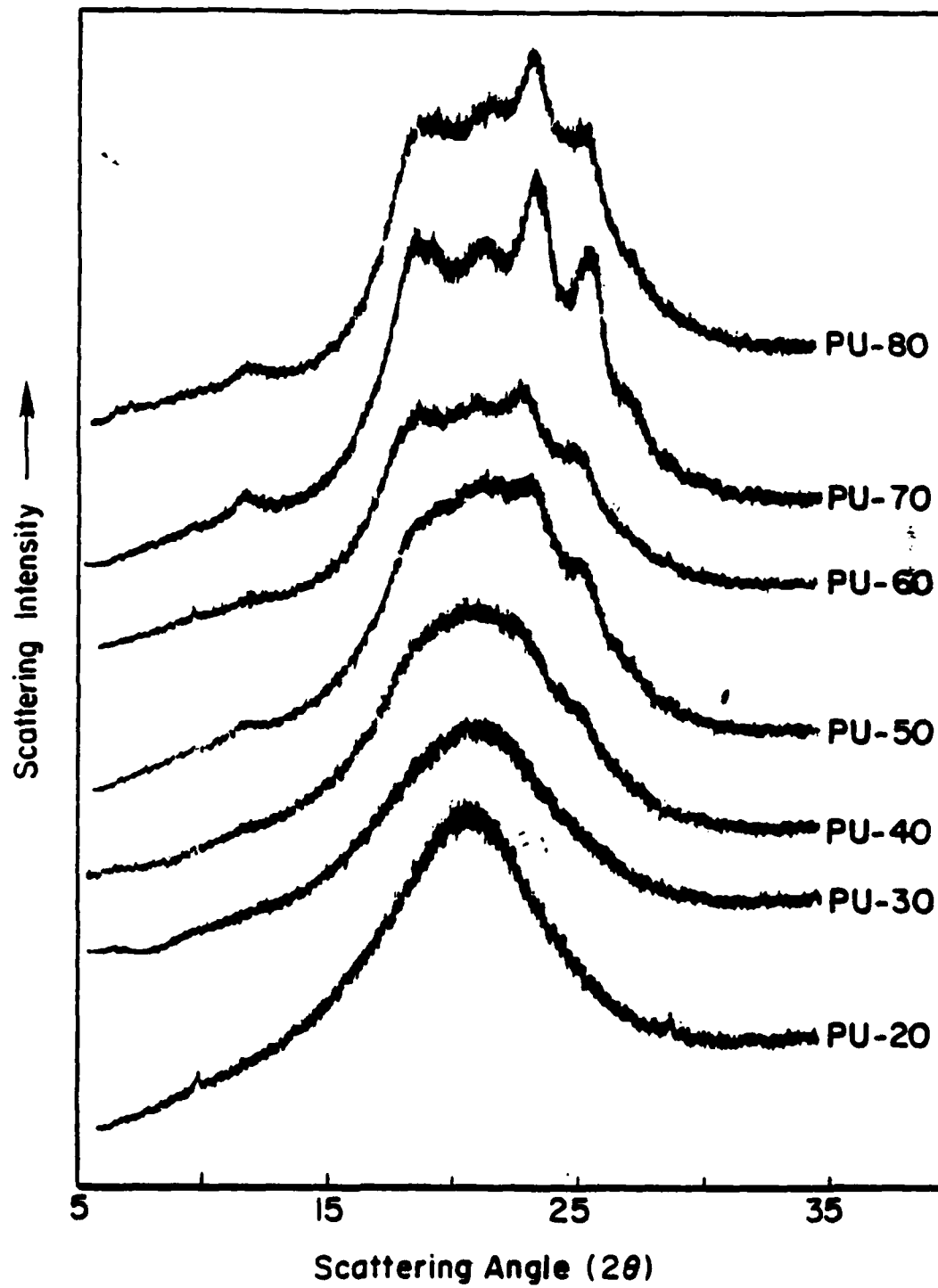


Fig 10